

A study of the optical properties of photopolymer Fabry–Perot microcavities by a dual-wavelength fibre optic architecture

Raquel L Heredero¹, Susana Martin¹,
Ramón Fernández de Caleyá¹, Antonio B Lobo Ribeiro²,
Francisco M Araújo², Luís A Ferreira², José Luís Santos^{3,4} and
Héctor Guerrero¹

¹ Laboratorio de Instrumentación Espacial—LINES, Área de Cargas Útiles e Instrumentación, División de Ciencias del Espacio, Instituto Nacional de Técnica Aeroespacial—INTA, 28850 Torrejón de Ardoz, Madrid, Spain

² MultiWave Networks Portugal, Lda., Portugal

³ Departamento de Física da Universidade do Porto, Rua do Campo Alegre, 687, 4169-007 Porto, Portugal

⁴ Unidade de Optoelectrónica e Sistemas Electrónicos, INESC Porto, Rua do Campo Alegre, 687, 4169-007 Porto, Portugal

Received 18 December 2001, in final form 10 April 2002, accepted for publication 22 April 2002

Published 20 June 2002

Online at stacks.iop.org/MST/13/1094

Abstract

We present a novel method to study the behaviour of the optical properties of photopolymer materials with temperature. The photopolymer is deposited on the tip of optical fibres by dip coating to fabricate low-finesse Fabry–Perot microcavities. The signal processing technique utilized to interrogate the cavity is based on the generation of two quadrature phase-shifted interferometric signals using two Bragg fibre gratings. This technique enables the determination of the values of the thermo-optical coefficient and the linear coefficient of thermal expansion of the photopolymer. The effectiveness of the processing technique is also exploited in the study of the dependence of the temperature sensitivity on the cavity thickness.

Keywords: optical fibre Fabry–Perot interferometer, photopolymer, temperature, optical properties

1. Introduction

Research on materials for optical applications has always been a matter of great interest. The behaviour of the optical path of materials under the action of several physical agents is an attractive topic for different areas in optics; such as holography, interferometry, characterization of coatings and development of new transducers for sensing.

Modulation of the refractive index of photopolymers results when the dye absorbs a photon in the presence of an electron donor, producing polymerization. Therefore,

photopolymers are promising candidates for alternative optical recording materials in holography and nonlinear optics [1–3]. These materials have excellent diffraction efficiency and consequently they are also suitable for applications in optical devices such as high-density storage and optical data processing. For all these reasons, the optical characterization of these materials is highly desirable.

It is well known that the environmental conditions and history of a polymer can drastically influence its morphology and material properties. In particular, relative humidity (RH) and temperature have a strong influence on the polymer's

properties [4]. Photopolymers that undergo polymerization generally present poor stability when exposed to light, both before and after recording. The investigation of polymers' refractive index and thickness variations is, in this sense, very interesting since these parameters turn out to be fundamental for holographic recording.

In this work, we have studied the thermal behaviour of the optical path of a photopolymer based on polyvinyl alcohol (PVA) after exposure to UV light. The photopolymer studied here shows several advantages: being a dry layer, it permits easy handling, it can be prepared in a straightforward manner and it has the important feature of being self-developed, which allows processing *in situ*. Finally, this material exhibits good stability after fabrication and is non-volatile [2].

Polymer materials have been deposited on the tip of optical fibres with different shapes for the fabrication of microlenses [5]. We present a novel low-finesse Fabry–Perot interferometer (LFFPI) based on photopolymer growth. The photopolymer microcavity is grown on the tip of a single-mode fibre by the dip-coating technique. The transfer function of the LFFPI can be approximated to that of the double-beam interferometer since the reflectivity of the interface fibre-transducer medium is typically small [6,7]. The interferometric optical signal from the LFFPI contains in its phase the information about the physical parameter acting on the optical path difference (OPD) of the cavity. When its length exceeds the coherence length of the light source negligible interference occurs at the output of the LFFPI. In this case, it is necessary to have a compensating receiving interferometer in order to recover the phase changes induced by the measurand. This technique, designated white light interferometry (WLI), has been extensively used to interrogate LFFPI projected for the measurement of several physical parameters, such as static and dynamic strains [8], pressure and temperature [9], electric field [10] and electrical current [11]. However, there are situations where the cavity length is smaller than the coherence length of the light source. In these cases the WLI technique is not applicable and an alternative process to interrogate the LFFPI is needed. One well proved solution consists in the generation of two quadrature phase-shifted interferometric signals [12]. This can be achieved in several ways and, as examples, we can point out the following: the utilization of two modes of a multimode laser diode [13,14], the implementation of single-mode laser diode frequency switching [15] and the utilization of two cavities with a differential length that accomplish the quadrature condition [16]. In this work, the scheme of generating two quadrature phase-shifted interferometric signals is utilized to interrogate the cavity. These signals are obtained through a new processing technique based on utilization of two fibre Bragg gratings (FBGs) [17].

The optical properties of PVA-based photopolymer were studied for temperature variation. The proposed technique allows one to obtain the linear coefficient of thermal expansion and the temperature coefficient of the refractive index of the material. The configuration proposed may also be used to develop a fibre optic temperature sensor since LFFPI are an adequate choice when a physically small optical sensor with high sensitivity is required.

2. Theory

The interferometric transfer function of the light reflected from a low-finesse Fabry–Perot cavity has the following well known approximation [7]:

$$I(\lambda) = I_0[1 + \Gamma \cos \phi]. \quad (1)$$

In this expression, I_0 is the average optical power reaching the detector, Γ is the fringe visibility of the cavity and ϕ is the interferometric phase for a reflective LFFPI which is given by

$$\phi(\lambda_0) = \frac{4\pi}{\lambda_0} \text{OPD} = \frac{2\pi}{\lambda_0} 2n_c L \quad (2)$$

where λ_0 is the peak wavelength of the optical source (assumed spectrally symmetric), and $\text{OPD} = 2n_c L$ is the optical path difference of the reflective cavity, with L denoting its physical length and n_c the refractive index of the intracavity medium. Therefore, information about the behaviour of the optical properties of the material that fills the cavity can be found in the optical phase of the signal. The optical phase changes are due to modifications in the wavelength, the thickness of the microcavity and/or refractive index of the medium.

The phase difference between two signals with wavelengths λ_1 and λ_2 can then be written as

$$\Delta\phi = 4\pi n_c L \left(\frac{1}{\lambda_1} - \frac{1}{\lambda_2} \right). \quad (3)$$

The two outputs, corresponding to each wavelength, will be in quadrature when separation between λ_1 and λ_2 equals

$$\Delta\lambda \approx \frac{\lambda_0^2}{8n_c L} (2m + 1); \quad m = 0, 1, \dots \quad (4)$$

where the following approximation was considered: $\lambda_1 \lambda_2 \approx \lambda_0^2$. Therefore, to interrogate a given microcavity it is possible, in most practical situations, to select two FBGs with resonant wavelengths that satisfy (4) in order to have access to two quadrature interferometric signals. Detecting each of these signals individually, we get

$$\begin{aligned} V_1(\phi) &= V_{10}(1 + \Gamma_1 \cos \phi) \\ V_2(\phi) &= V_{20} \left\{ 1 + \Gamma_2 \cos \left[\phi + (2m + 1) \frac{\pi}{2} \right] \right\} \\ &= V_{20}(1 + \Gamma_2 \sin \phi) \end{aligned} \quad (5)$$

where V_{i0} ($i = 1, 2$) is the average output voltage related to the average optical power in each channel and detector gain and Γ_{i0} ($i = 1, 2$) is the visibility of the signals.

Tuning the global gain to have $V_{10}\Gamma_1 = V_{20}\Gamma_2$, allows one to recover the interferometric phase through the following relation:

$$\phi = \tan^{-1} \left(\frac{V_2 - V_{20}}{V_1 - V_{10}} \right). \quad (6)$$

The unambiguous phase from $-\pi$ to π can be calculated using the above equation and one of the signals in (5).

As stated previously, in this work, the LFFPI is based on a photopolymer material deposited on the tip of an optical fibre by the dip-coating technique. Polymers present a

particular interesting characteristic temperature, called the glass transition temperature, T_g . T_g describes the temperature at which the forces holding together the distinct components of the amorphous polymer solid are overcome. Above T_g , these components are able to undergo viscous flow. Below T_g , linear variation of the refractive index and the thickness of the photopolymer film with temperature can be assumed:

$$\begin{aligned} n_c(T) &= n_{c0} + \kappa(T - T_0) \\ L(T) &= L_0 + \alpha L_0(T - T_0) \end{aligned} \quad (7)$$

where n_{c0} and L_0 are the reference values at $T = T_0$, κ is the thermo-optical coefficient and α is the linear coefficient of thermal expansion.

By substituting (7) into (2), the temperature dependency of the optical phase can be expressed by

$$\begin{aligned} \phi(T) &= \frac{4\pi}{\lambda_0} [n_{c0} + \kappa(T - T_0)][L_0 + \alpha L_0(T - T_0)] \\ &= \phi_0 + \nu_\phi(T - T_0) + \xi_\phi(T - T_0)^2 \quad \text{for } (T < T_g). \end{aligned} \quad (8)$$

where

$$\begin{aligned} \phi_0 &= \frac{4\pi}{\lambda_0} n_{m0} L_0 \\ \nu_\phi &= \frac{4\pi}{\lambda_0} (n_{m0} \alpha + \kappa) L_0 \\ \xi_\phi &= \frac{4\pi}{\lambda_0} \alpha \kappa L_0. \end{aligned}$$

As will be shown in what follows, the coefficient ξ_ϕ is much smaller than ν_ϕ for a given L_0 and therefore the quadratic dependence of the phase with temperature may be neglected. Considering this, the relationship between the optical phase and temperature can be written as

$$\phi(T) \approx \phi_0 + \nu_\phi(T - T_0). \quad (9)$$

Equation (9) yields information about the behaviour of optical properties of the photopolymer material under the action of temperature. In fact, from ν_ϕ it is possible to calculate the relation between coefficients α and κ for the photopolymer used.

The term ν_ϕ in (9) gives the temperature sensitivity obtained with photopolymer cavities of thickness L_0 . Sensitivity enhancement can be achieved with longer cavities, as will be confirmed in this work. Equation (9) indicates that, for a given cavity length, the sensitivity is inversely proportional to λ . Considering that, it was decided to illuminate the LFFPI with radiation having a wavelength around 830 nm.

3. Fabrication and characterization of the LFFPI

The material under study is a dry and consistent photopolymer containing a monomer, an electron donor and a sensitizing dye. Local polymerization is initiated when the dye absorbs a photon and reacts with the electron donor to produce a free radical. The local refractive index is altered wherever polymerization occurs.

The photopolymer used in this work consists of a polymer matrix (PVA) acting as a binder, two acrylamide

monomers (bisacrylamide and acrylamide), an electron donor (triethanolamine (TEA)) and a dye sensitizer (Rose Bengal). The photopolymer was prepared as follows: 6.75 g of PVA from FLUKA (degree of hydrolyzation 87% and number averaged molecular weight $M_n \sim 130\,000$) were added to 45 ml of deionized H_2O and mixed well. The monomer solution consists of 3.0 g of acrylamide and 0.8 g of bisacrylamide in 7.5 ml of deionized H_2O . When the monomer solution is totally dissolved, 2.5 ml of TEA is added to the monomer solution. Afterwards, 8 ml of this dissolution is added to the PVA solution and stirred until complete homogeneity is achieved. 2.5 ml of the Rose Bengal photoinitiator is added to the previous solution in darkness to avoid photopolymerization. This final dissolution is left stirring at a low speed to avoid bubble formation.

The refractive index of the prepared PVA photopolymer was measured at 589 nm with an Abbe refractometer (Bellingham & Stanley Ltd, Model 60/H) as being $n_{c0} = 1.525$ at $T_0 = 24.6^\circ C$. The glass transition temperature was also measured: by using a thermomechanical analyser (TMA 40, Mettler Toledo) at a rate of $10^\circ C \text{ min}^{-1}$ the value $T_g = 70^\circ C$ was obtained.

In order to characterize the optical properties of this material under the action of temperature in a precise way, microcavities on the tip of optical fibres were fabricated. The photopolymer was grown on the tip of the fibre by dip coating. The thickness of the film depends mainly on the density of the dissolution and the speed of immersion. The fibre tip was cut perpendicular to the fibre axis. Before coating the fibre tip, it was previously cleaned with deionized water, acetone and finally ethanol. The fibre was dipped into the photopolymer dissolution at a speed of 11.9 cm min^{-1} . After each immersion, the fibre was left to dry in air, at a controlled temperature of $\sim 19^\circ C$, for about 20 min. After the final immersion, the fibre tip was irradiated with UV light for ~ 45 min to activate polymerization of the monomers. These microcavities present good consistency under mechanical action and uniformity between interfaces from several immersions.

The adherence and thickness of the photopolymer on the fibre were analysed by scanning electron microscopy (SEM). As shown in figure 1, the photopolymer was effectively adhered to the tip of the fibre, and the thickness values measured were $\sim 4.5 \mu\text{m}$ (figure 1(a)), $\sim 9.55 \mu\text{m}$ (figure 1(b)), $\sim 21.9 \mu\text{m}$ (figure 1(c)) and $\sim 35.0 \mu\text{m}$ (figure 1(d)) for a sequence of one, two, five and seven immersions, respectively. The average thickness of the films grown on the tip of the fibre was $\sim 4.5 \mu\text{m}$ per dip and, therefore, good control of this parameter can be achieved.

In order to study the temperature behaviour of these LFFPI cavities, a six-immersion fibre was chosen. To determine the OPD of the cavity, a spectroscopic characterization was carried out (figure 2). The light source used was a pigtailed superluminescent diode (SuperlumSLD-361/A, $\lambda_0 \approx 826.5 \text{ nm}$, spectral width of $\sim 20.5 \text{ nm}$). The optical power injected into the fibre was $\sim 2 \text{ mW}$. The free spectral range (FSR) of a Fabry-Perot interferometer working in reflection describes the separation of the spectral peaks in its transfer function and is given by

$$\text{FSR} = \frac{\lambda_0^2}{\text{OPD}}. \quad (10)$$

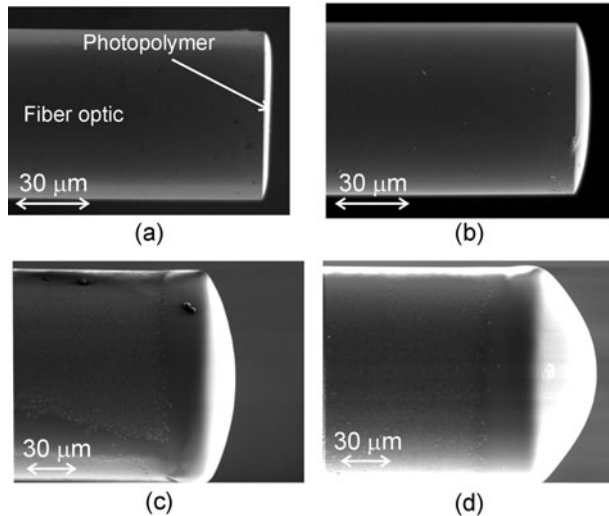


Figure 1. SEM micrographs of photopolymer fibre tips fabricated with different a number of immersions: (a) one immersion, (b) two immersions, (c) five immersions and (d) seven immersions.

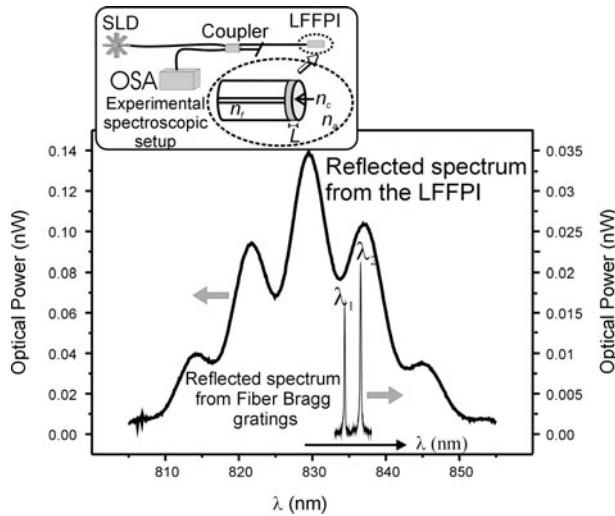


Figure 2. Spectrum reflected from the LFFPI. The spectral signatures of the FBGs corresponding to a quadrature situation ($\Delta\lambda \sim 2.17$ nm) are also shown. The scheme of the experimental spectroscopic set-up is also included.

Figure 2 also shows the spectrum arriving at the optical spectrum analyser (OSA), from which the FSR of the LFFPI can be determined as ~ 8.4 nm. An OPD for the photopolymer cavity of ~ 40.7 μm emerges from (10). Considering that for the temperature of measurement ($T_0 = 24.6^\circ\text{C}$) the refractive index of the photopolymer is $n_{c0} = 1.525$, the thickness of the cavity can be calculated as $L_0 \sim 26.75$ μm . Since the coherence length of the light reflected by the FBGs is of the order of several millimetres, the two main waves generated at the cavity interfaces mix coherently. Therefore, the use of an additional receiving interferometer to recover the optical phase from the microcavity is not necessary as in WLI techniques.

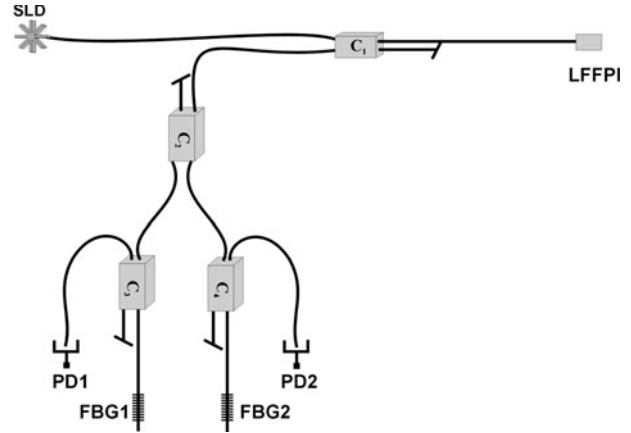


Figure 3. Experimental fibre optic set-up.

4. Experimental results and discussion

Complete cycles of temperature were carried out to study the optical properties of this material. The experimental set-up implemented to measure the dependence of the cavity interferometric phase with temperature is shown in figure 3. Light from the superluminescent diode illuminated the Fabry–Perot cavity through a 50:50 coupler (C_1). Light reflected back is then guided to both FBGs via another 50:50 coupler (C_2). The optical signals from the two spectral discriminators reach two photodetectors through couplers C_3 and C_4 (also 50:50). The average optical power arriving at one of the couplers was ~ 4 nW, while for the other this value was $\sim 50\%$ higher due to smaller losses in the optical fibre link. In equation (6) the corresponding voltage signals were processed using LabView™ software in order to obtain the interferometric phase.

As mentioned previously, the history of a polymer can drastically influence its optical properties. In addition, the properties of polymers are temperature rate dependent. Therefore, several complete temperature cycles were performed at different rates and for different periods of time.

The temperature characterization of the microcavities was performed with a six-immersion fibre with $L_0 \sim 26.75$ μm . To interrogate the LFFPI, two FBGs were used as spectral discriminators to obtain two quadrature phase-shifted signals. Their resonance wavelengths were chosen as $\lambda_{B1} = 834.4$ and $\lambda_{B2} = 836.5$ nm (see figure 2) which means a wavelength difference of $\Delta\lambda = 2.1$ nm, in order to work in the quadrature point according to (4). Figure 4 shows the evolution of the optical phase during a complete cycle of heating and cooling. The heating rate was $4.7^\circ\text{C min}^{-1}$ and cooling was performed following a typical exponential decay function. As can be observed in this figure, the interferometric method used in the experiment clearly reveals a hysteretic dependence between the microcavity OPD and the temperature. The hysteresis behaviour is intensified when the cooling process is very slow. Slow cooling provides a great amount of crystallization and so variation of the thickness of the photopolymer is much smaller as for crystalline solids.

Rapid quenches of the photopolymer yield a highly amorphous state. This feature of the photopolymer is shown

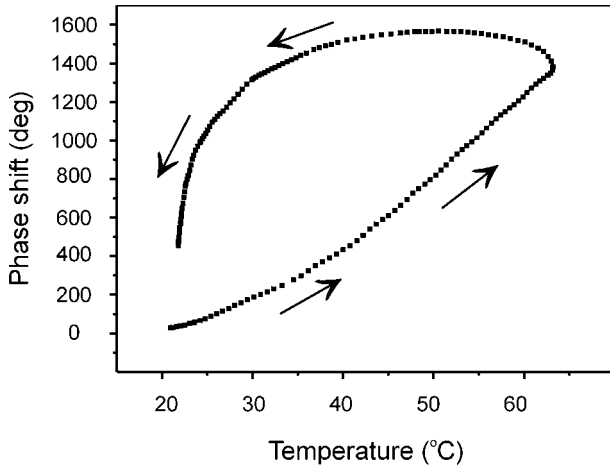


Figure 4. Interferometric phase shift versus temperature for a fibre with $L_0 \sim 26.75 \mu\text{m}$.

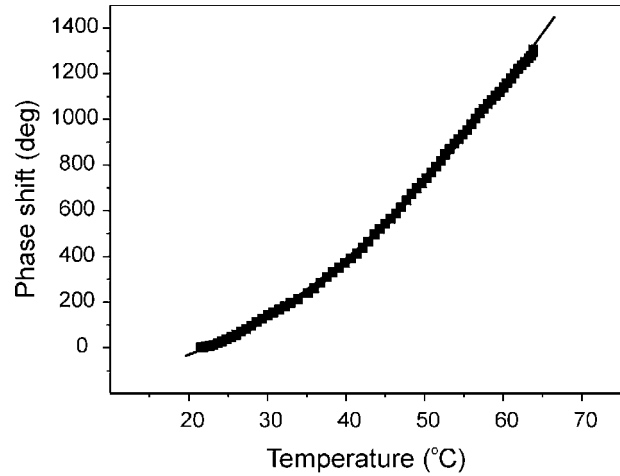


Figure 6. The phase-shift with temperature during the heating process.

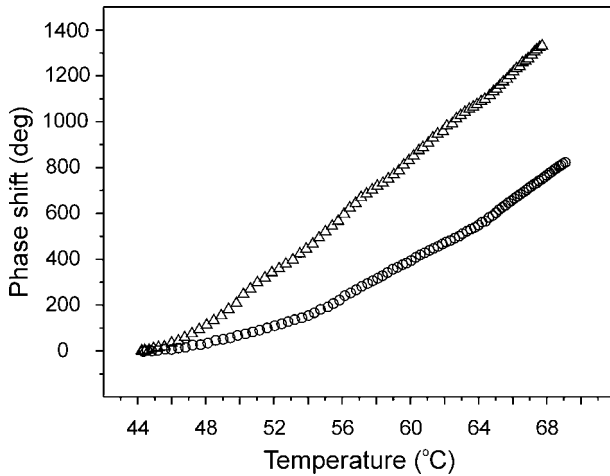


Figure 5. Optical phase response after a rapid quenching of the photopolymer film.

in figure 5. Open circles represent the optical phase shift for a heating cycle of $0.53^\circ\text{C min}^{-1}$ and a microcavity with $L_0 \sim 35 \mu\text{m}$. After that, the microcavity was left to cool down at room atmosphere. Then, the photopolymer film experienced a rapid quench of 0.24°C in 0.5 s ($-28.7^\circ\text{C min}^{-1}$). Subsequent heating relieves stresses for the chains of the polymer. Therefore, the variation of the optical phase for a consequent heating process at the same rate as the first one (represented by open triangles in figure 5) is much higher due to relaxation of the chains.

Figure 6 shows the relation between the optical phase and temperature during the heating process ($4.7^\circ\text{C min}^{-1}$) from the same microcavity as presented in figure 4. The data fits to the second-order polynomial fit according to (8).

Considering the linear approximation (9), the slope of $\sim 34^\circ\text{C}$ for the cavity under investigation is indicative of the large temperature optical response of photopolymer-based LFFPIs. In order to calculate the thermal coefficients of this material, several measurements at the same heating and cooling rate were carried out with different thickness cavities. A spectroscopic analysis was performed for each fibre and its associated cavity in order to evaluate the wavelength shift of

the two FBGs required for quadrature operation. The relation between the temperature sensitivity and the thickness of each microcavity L_0 is represented in figure 7. A linear relationship between ν_ϕ and L_0 can be observed, in fair agreement with equation (9). Enhancement of the temperature sensitivity can be achieved by larger microcavities. The sensitivity enhancement factor, ν_ϕ , is $\sim 1.1^\circ\text{C}$ for each micron of photopolymer deposited on the tip of the fibre. This value, when combined with (9), permits one to obtain

$$n_{c0}\alpha + \kappa = 1.27 \times 10^{-3} \text{ }^\circ\text{C}^{-1}. \quad (11)$$

The signal from our reflective LFFP photopolymer microcavity results from recombination of only the first-order reflected beam from the fibre end, with the first-order reflected beam from the surface of the material deposited on the tip of the fibre. These beams depend mainly on the reflection coefficients between the fibre optic and photopolymer, and between the photopolymer and air, respectively. The reflection coefficients are given by the well known Fresnel formulae [18]. The mean optical power received at both photodetectors (I_0 in (1)) comes from the sum of both beams, and therefore depends mainly on the variation of the refractive index of the fibre and of the photopolymer with temperature. The same occurs with the visibility of the signals that reach the photodetectors (Γ in (1)). It is important to note that the mean optical power is also dependent on the absorption of light as it passes through the photopolymer. This absorption is related to the refractive index of the material.

When the temperature increases, the thickness of the microcavity is incremented. This provokes a diminution of the material density and consequently of the refractive index. Therefore, both parameters contribute in opposite directions in the temperature phase shift.

In our measurements, the mean optical power changes $\sim 1\%$ and the visibility varies $\sim 8\%$ for the temperature range measured. This fact means that the variation of the refractive index of the photopolymer cavity is low. Therefore, the optical phase shift during heating is mainly due to the expansion of the photopolymer.

Measurements represented in figure 7 can be fitted with $\alpha = 10 \times 10^{-4} \text{ }^\circ\text{C}^{-1}$ and $\kappa = -1.5 \times 10^{-4} \text{ }^\circ\text{C}^{-1}$. By

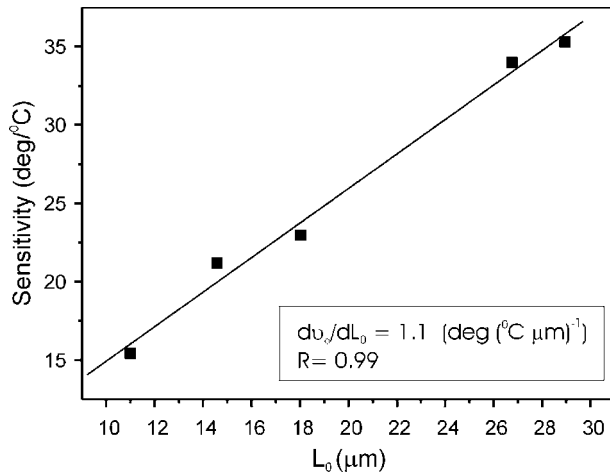


Figure 7. The temperature phase sensitivity of photopolymer cavities with different thickness values.

substituting these values in equation (8), $\xi_\phi = -1.3 \times 10^{-4} \text{ } ^\circ\text{C}^{-2}$ for each micron is obtained. This coefficient is four orders of magnitude smaller than ν_ϕ and therefore approximation (9) is well justified.

The value for the linear coefficient of thermal expansion α differs from the value obtained for the characterization of a bulk sample by the thermomechanical analyser (TMA 40, Mettler Toledo). This is due to the fact that the way the photopolymer molecules are arranged in a solid is an important factor in determining the properties of the polymer. In fact, the value for the thermo-optical coefficient is in agreement with the value obtained when the same photopolymer was deposited onto side-polished single-mode fibres [19].

5. Conclusion

In conclusion, the fibre architecture proposed here provides a useful configuration to study the optical properties of different materials deposited on the tip of an optical fibre. To interrogate the cavity and recover the relevant information, the effectiveness of a new approach based on the utilization of two FBGs to generate two quadrature phase-shifted interferometric signals was reported. This scheme permits one to estimate both the thermo-optical coefficient and the linear coefficient of thermal expansion for the material under investigation.

In principle, the system can also be used as a fibre optic sensor for high-sensitivity temperature measurements offering all the advantages of this type of sensor; the main advantages being electromagnetic immunity and small physical dimensions. In fact, the thickness of the photopolymer

on the tip of the fibre can be made greater than the values obtained using other deposition techniques presented in the literature. As shown before, this feature yields longer OPDs and, therefore, larger interferometric sensitivity to temperature. However, the existence of hysteresis can limit this application.

Acknowledgments

First, the author would like to thank F del Monte for his interesting discussions. He also gratefully acknowledges the contributions of M Dahlem with the LabView software and J Álvarez Alba with the SEM measurements.

This work has been partially supported by *Dirección General de Investigación de la Comunidad de Madrid*.

References

- [1] Beléndez A, Fimia A, Carretero L and Mateos F 1995 *Appl. Phys. Lett.* **67** 3856–8
- [2] Martin S, Leclere P E L G, Toal V and Lion Y F 1994 *Opt. Eng.* **33** 3942–7
- [3] Martin S, Feely C A and Toal V 1997 *Appl. Opt.* **36** 5757–68
- [4] Bicerano J 1996 *Prediction of Polymer Properties* (New York: Marcel Dekker)
- [5] Bachelot R, Ecoffet C, Deloeil D, Royer P and Loughnot D J 2001 *Appl. Opt.* **40** 5860–71
- [6] Chen S, Palmer AW and Grattan K T V 1993 *Pure Appl. Opt.* **2** 429–35
- [7] Santos J L, Leite A P and Jackson D A 1992 *Appl. Opt.* **31** 7361–6
- [8] Sirkis J, Berkoff T A, Jones R T, Singh H, Kersey A D, Friebele E J and Putnam M A 1995 *J. Lightwave Technol.* **13** 1256–63
- [9] Rao Y J, Jackson D A, Jones R and Shannon C 1994 *J. Lightwave Technol.* **12** 1685–95
- [10] Priest T S, Scelsi G B and Woolsey G A 1997 *Appl. Opt.* **36** 4505–8
- [11] Heredero R L, Fernández de Caleyá R, Guerrero H, Los Santos P, Acero M C and Esteve J 1999 *Appl. Opt.* **38** 5298–305
- [12] Kersey A D, Jackson D A and Corke M 1982 *Electron. Lett.* **18** 392–3
- [13] Ezbiri A and Tatam R P 1995 *Opt. Lett.* **20** 1818–20
- [14] Murphy K A, Gunther M F, Vengsarkar A M and Claus R O 1991 *Opt. Lett.* **16** 273–5
- [15] Kersey A D, Jackson D A and Corke M 1983 *Electron. Lett.* **19** 102–3
- [16] Santos J L and Jackson D A 1991 *Opt. Lett.* **16** 1210–12
- [17] Dahlem M, Santos J L, Ferreira L A and Araújo F M 2001 *IEEE Photonics Technol. Lett.* **13** 990–2
- [18] Born M and Wolf E 1980 *Principles of Optics* (Oxford: Pergamon) ch 1
- [19] Álvarez-Herrero A, Guerrero H, Belenguer T and Levy D 2000 *IEEE Photonics Technol. Lett.* **12** 1043–5